

Somatic Ca^{2+} transients do not contribute to inspiratory drive in preBötzinger Complex neurons

Consuelo Morgado-Valle¹, Luis Beltran-Parrazal², Marino DiFranco³, Julio L. Vergara³ and Jack L. Feldman¹

¹Systems Neurobiology Laboratory, Department of Neurobiology, David Geffen School of Medicine at UCLA, University of California Los Angeles, Box 951763, Los Angeles, CA 90095-1763, USA

²Division of Head and Neck Surgery, David Geffen School of Medicine at UCLA, University of California Los Angeles, Los Angeles, CA 90095-1794, USA

³Department of Physiology, David Geffen School of Medicine at UCLA, University of California Los Angeles, Los Angeles, CA 90095-1751, USA

PreBötzinger Complex (preBötC) neurons are postulated to underlie respiratory rhythm generation. The inspiratory phase of the respiratory cycle *in vitro* results from preBötC neurons firing synchronous bursts of action potentials (APs) on top of 10–20 mV, 0.3–0.8 s inspiratory drive potentials. Is the inspiratory drive in individual neurons simply the result of the passive integration of inspiratory-modulated synaptic currents or do active processes modulate these currents? As somatic Ca^{2+} is known to increase during inspiration, we hypothesized that it affects inspiratory drive. We combined whole cell recording in an *in vitro* slice preparation with Ca^{2+} microfluorometry to detect single inspiratory neuron somatic Ca^{2+} transients with high temporal resolution ($\sim\mu\text{s}$). In neurons loaded with either Fluo-4 or Oregon Green BAPTA 5 N, we observed Ca^{2+} transients associated with each AP. During inspiration, significant somatic Ca^{2+} influx was a direct consequence of activation of voltage-gated Ca^{2+} channels by APs. However, when we isolated the inspiratory drive potential in active preBötC neurons (by blocking APs with intracellular QX-314 or by hyperpolarization), we did not detect somatic Ca^{2+} transients; yet, the parameters of inspiratory drive were the same with or without APs. We conclude that, in the absence of APs, somatic Ca^{2+} transients do not shape the somatic inspiratory drive potential. This suggests that in preBötC neurons, substantial and widespread somatic Ca^{2+} influx is a consequence of APs during the inspiratory phase and does not contribute substantively to the inspiratory drive potential. Given evidence that the Ca^{2+} buffer BAPTA can significantly reduce inspiratory drive, we hypothesize that dendritic Ca^{2+} transients amplify inspiratory-modulated synaptic currents.

(Received 3 April 2008; accepted after revision 14 July 2008; first published online 17 July 2008)

Corresponding author C. Morgado-Valle: Department of Neurobiology, David Geffen School of Medicine at UCLA, Box 951763, Los Angeles, CA 90095-1763, USA. Email: cmorgado@mednet.ucla.edu

PreBötzinger Complex (preBötC) neurons in the brainstem underlie respiratory rhythm generation *in vitro* (Smith *et al.* 1991; Feldman & Del Negro, 2006) and are essential for breathing in awake adult rats *in vivo* (Gray *et al.* 2001; Tan *et al.* 2008). The inspiratory phase of the respiratory cycle *in vitro* results from preBötC neurons firing a synchronous burst of action potentials (APs) on top of a 10–20 mV, 0.3–0.8 s depolarization (inspiratory drive potential). Although preBötC neurons express burst-promoting currents such as I_{NaP} and I_{CAN} (Del Negro *et al.* 2002; Pena *et al.* 2004), less than 10% are intrinsic pacemaker neurons (Del Negro *et al.* 2005) and the vast majority are non-pacemaker neurons requiring excitatory synaptic input to burst rhythmically. In these non-pacemaker preBötC neurons, the mechanisms

determining the inspiratory drive potential are not fully known. AMPA receptor-mediated synaptic transmission is essential for generation of inspiratory currents (Funk *et al.* 1993; Greer *et al.* 1991), whereas that mediated by NMDA receptors, at least *in vitro*, does not contribute significantly (Funk *et al.* 1997; Morgado-Valle & Feldman, 2007). A class of non-selective cationic channels activated by elevated cytosolic $[\text{Ca}^{2+}]_i$ (Vennekens & Nilius, 2007; Crowder *et al.* 2007) are postulated to play an essential role in shaping the inspiratory drive potential (Pace *et al.* 2007).

In neurons, changes in $[\text{Ca}^{2+}]_i$ regulate different events over time scales from less than milliseconds, e.g. triggering of neurotransmitter release at presynaptic terminals, to seconds, e.g. during bursting activity, to

hours, days or longer (Augustine *et al.* 2003). The spatial and temporal characteristics of Ca^{2+} transients are shaped by Ca^{2+} influx through voltage- and ligand-gated channels, intracellular release and buffering. Interestingly, intrinsic Ca^{2+} buffering in preBötC neurons may be limited (Alheid *et al.* 2002), suggesting that Ca^{2+} transients could play a role in generation of respiratory rhythm and pattern. The contribution of Ca^{2+} and Ca^{2+} -dependent conductances to membrane potential fluctuations in respiratory neurons has been studied both *in vivo* (Pierrefiche *et al.* 1995, 1999; Haji & Ohi, 2006) and *in vitro* (Onimaru *et al.* 1996; Elsen & Ramirez, 1998; Mironov & Richter, 1998). Whereas most of these studies established the presence of Ca^{2+} and Ca^{2+} -dependent currents in respiratory neurons, none focused explicitly on the role of Ca^{2+} in determining the inspiratory drive potential. Optical imaging studies using cell permeant forms of Ca^{2+} -sensitive dyes reveal Ca^{2+} transients during inspiration in active preBötC neurons (Koshiya & Smith, 1999; Frermann *et al.* 1999; Barnes *et al.* 2007; Funke *et al.* 2007; Mironov, 2008) and in respiratory-modulated hypoglossal motoneurons (Ladewig & Keller, 2000). However, these studies were done in active preparations where neurons were firing APs during inspiration; thus, whether Ca^{2+} transients in any given neuron resulted from its (subthreshold) inspiratory drive potential, APs, or both was not addressed. Here we characterize at high temporal resolution somatic Ca^{2+} dynamics in preBötC neurons to test the hypothesis that somatic Ca^{2+} increases with inspiratory onset and contributes to inspiratory drive. We used whole cell recording and a photodiode system that resolves Ca^{2+} signals with high temporal resolution (67 kHz) to detect single neuron somatic Ca^{2+} signals in neonatal rat medullary slice preparations while recording simultaneously respiratory-related rhythmic hypoglossal nerve activity ($\int \text{XIIIn}$). We intracellularly applied the Ca^{2+} sensitive dyes Fluo-4 or Oregon Green BAPTA 5N (OGB5N) to resolve somatic Ca^{2+} signals. Our principal result is that during inspiration somatic Ca^{2+} transients are a direct consequence of APs, but this influx does not affect the inspiratory drive potential. We conclude that in preBötC neurons, somatic Ca^{2+} transients are a consequence and not a modulator of bursting. We hypothesize that dendritic Ca^{2+} transients modulate synaptically mediated inspiratory drive currents.

Methods

Medullary slice preparation

Experiments were performed on neonatal rat transverse brainstem slices that generate respiratory-related motor output (Smith *et al.* 1991). The Office for the Protection of Research Subjects, University of California Research

Committee approved all protocols. Briefly, neonatal rats (0–3 days old) were anaesthetized with isoflurane and decerebrated, and the neuroaxis was isolated. The cerebellum was removed and the brainstem sectioned serially in transverse plane using a VT-1000 Vibratome (Vibratome, St Louis, MO, USA) until neuroanatomical landmarks, i.e. nucleus ambiguus, inferior olive, were visible. A transverse slice (550 μm) containing the preBötC was cut (Ruangkittisakul *et al.* 2006). The dissection was performed in an artificial cerebrospinal fluid (ACSF) containing (in mM): 128 NaCl, 3 KCl, 1.5 CaCl_2 , 1 MgSO_4 , 23.5 NaHCO_3 , 0.5 NaH_2PO_4 and 30 glucose, bubbled with 95% O_2 –5% CO_2 at 27°C. The slice was transferred to a 1 ml recording chamber and anchored using a platinum frame and a grid of nylon fibres. The chamber was mounted to a fixed-stage microscope and perfused with ACSF (6 ml min^{-1}).

Electrophysiological recording

Rhythmic respiratory-related motor output was recorded from the XIIIn using fire-polished glass suction electrodes and a differential amplifier. To obtain a robust and stable rhythm, ACSF K^+ concentration was elevated to 9 mM and slices were perfused for 30 min before any experimental manipulation. XIIIn activity was amplified, bandpass filtered (0.3–1 kHz), rectified and integrated ($\tau = 20$ ms; $\int \text{XIIIn}$). Whole-cell patch-clamp recordings were performed using an Axopatch 200A amplifier (Molecular Devices, Sunnyvale, CA, USA) in current-clamp mode. Inspiratory neurons from preBötC were visualized using infrared-enhanced differential interference contrast videomicroscopy. Electrodes were pulled from borosilicate glass (o.d., 1.5 mm; i.d., 0.86 mm) on a horizontal puller. Electrodes were filled with solution containing (in mM): 140 potassium gluconate, 5 NaCl, 10 HEPES, 0.1 CaCl_2 , 1.1 EGTA, 2 Mg-ATP (pH 7.3). Series resistance (R_s) and cell capacitance (C_M) were estimated under voltage-clamp conditions and compensated as previously described (Morgado-Valle & Feldman, 2007). Electrophysiological signals were acquired digitally at 4–20 kHz using pCLAMP software and a Digidata 1320 AD/DA board (Molecular Devices, Sunnyvale, CA, USA) after low-pass filtering.

Drugs

Drugs obtained from Sigma Chemical Co. (St Louis, MO, USA) were bath applied at the following concentrations: 20 nM TTX, 10 μM nimodipine. QX-314 at 20 mM was applied intracellularly via patch solution. ω -conotoxin GVIA (500 nM) and ω -agatoxin IVA (50 nM) were obtained from Tocris (Ellisville, MO, USA) and Alamone Laboratories (Jerusalem, Israel), respectively.

Ca²⁺ transient detection

500 μM of either the high affinity Ca²⁺ dye Fluo-4 (pentapotassium salt, cell-impermeant form) or the low affinity Ca²⁺ dye Oregon Green BAPTA 5N (OGB5N, hexapotassium salt, cell-impermeant form), both from Molecular Probes (Eugene, OR, USA), were included in the intracellular pipette. The system to detect fluorescence from Ca²⁺-sensitive dyes consisted of an upright microscope (DMLFS, Leica, Wetzlar, Germany) equipped for epi-fluorescence with a LED (LUXEON LXHLNB98, 480–485 nm, Quadica Developments Inc., Brantford, Ontario, Canada), a 63 \times objective (HCX APO 0.90 NA, Leica), an I3 filter cube (Leica I3, excitation filter: 450–490 nm; dichromatic mirror: 510 nm; suppression long pass filter: 515 nm) and a photodiode (UV-001; United Detector Technology, Hawthorne, CA, USA) mounted at the image plane in the top port of the microscope (Kim & Vergara, 1998). The photodiode current was amplified using an Axopatch-1B (Molecular Devices), filtered (1–2 kHz) and digitized at 67 kHz sampling rate using a Digidata 1322A. Fluorescence signals were recorded from a region of illumination centred on the active area (0.8 mm²) of the photodiode. LED illumination and photodiode current acquisition onset were synchronized and controlled via TTL pulses from Clampex with a custom-made acquisition protocol. Ca²⁺ dye *in vitro* calibrations (DiGregorio & Vergara, 1997) were performed using solutions with increasing [Ca²⁺] (from pCa 8 to pCa 3, i.e. from 10 nM to 1 mM). Calculated K_d values were 433 ± 6.4 nM ($n = 4$) and 38 ± 1.6 μM ($n = 3$) for Fluo-4 and OGB5N, respectively. $F_{\text{max}}/F_{\text{min}}$ ratios were 103 ± 10.5 and 43 ± 4.4 for Fluo-4 and OGB5N, respectively. For each dye, we determined the [Ca²⁺] detection threshold by calculating the minimal [Ca²⁺] change that resulted in a fluorescence change (in $\Delta F/F$) with a signal-to-noise ratio equal to 1, starting from a baseline at pCa 8. The detection threshold was ~ 60 nM and ~ 1.4 μM for Fluo-4 and OGB5N, respectively.

Data collection and analysis

Once whole-cell recording was established, 5–7 min were allowed for the Ca²⁺-sensitive dye to diffuse inside the neuron and for extracellular background fluorescence to be washed out. To test for dye effects on preBötC neuron properties, we recorded inspiratory neurons ($n = 5$) with Ca²⁺-sensitive dyes in the intracellular pipette for up to 1 h, during which no apparent changes in inspiratory drive amplitude, duration or number of APs were observed (data not shown). Only one experiment was performed per neuron/per slice. Custom-made software programmed in LabView (National Instruments, Austin, TX, USA) was used to calculate $\Delta F/F$. We considered as Ca²⁺

transients signals above a threshold set to 3 times the standard deviation of the mean baseline $\Delta F/F$. To test the variability between $\Delta F/F$ from spontaneous inspiratory bursts in different neurons, we calculated the variance among traces. No statistically significant differences were found among variance from neurons loaded with Fluo-4 or among variance from neurons loaded with OGB5N (data not shown). Igor Pro (Wave Metrics, Inc., Portland, OR, USA), Chart (ADInstruments, Colorado Springs, CO, USA), Origin (OriginLab Corporation, Northampton, MA, USA) and Microsoft Excel were used for data analyses. Results are expressed as means \pm S.E.M. ANOVA and Student's *t* test were used when appropriate.

Results

Ca²⁺ transients in response to evoked action potentials

Via patch-clamp electrodes placed under visual guidance at the soma, inspiratory preBötC neurons were loaded with Fluo-4 ($n = 82$) or with OGB5N ($n = 74$). Ca²⁺ transients in response to evoked APs were visualized in neuronal somas after injection of depolarizing current (I_{DC}) during the interburst interval, i.e. expiratory period. Given the high somatic to dendritic ratio of recorded areas, detected Ca²⁺ signals with a single photodiode were essentially somatic. In neurons loaded with Fluo-4, Ca²⁺ transients in response to evoked single APs (Fig. 1*Ab*) or trains of APs (Fig. 1*Ac–d*) had slow decay time constants. The peak transient $\Delta F/F$ ($(\Delta F/F)_{\text{peak}}$) increased with the number of APs (Fig. 1*B*). Ca²⁺ transients associated with each AP were more readily observable in neurons loaded with OGB5N (Fig. 1*D*, upper traces); during I_{DC} injection $(\Delta F/F)_{\text{peak}}$ remained constant regardless the number of evoked APs (Fig. 1*Db–d* and *E*). In inspiratory neurons loaded with Fluo-4, the single AP-evoked Ca²⁺ transient (Fig. 1*C*) had averaged $(\Delta F/F)_{\text{peak}} = 0.024 \pm 0.006$ and $\tau = 58.2$ ms, whereas neurons loaded with OGB5N had averaged $(\Delta F/F)_{\text{peak}} = 0.0087 \pm 0.0005$ and $\tau = 17.1$ ms (Fig. 1*F*). Thus, the increasing $\Delta F/F$ seen with Fluo-4 was the result of the slow kinetics of dye and did not reflect intracellular Ca²⁺ accumulation. The faster decay time of OGB5N allows better resolution of each individual AP, but it has the disadvantage of reporting larger changes in [Ca²⁺] than Fluo-4; therefore in some experiments we used Fluo-4 only.

In non-respiratory-modulated preBötC neurons loaded with either Fluo-4 ($n = 10$, Fig. 1*B*) or OGB5N ($n = 6$, Fig. 1*E*), $(\Delta F/F)_{\text{peak}}$ resulting from evoked APs fitted the same function as for inspiratory neurons, suggesting that the somatic Ca²⁺ transients during evoked APs were the same in all preBötC neurons regardless of their rhythmic phenotype *in vitro*.

Effect of Ca²⁺ channel blockers on Ca²⁺ transients and respiratory rhythm

In neurons loaded with Fluo-4 we investigated the contribution of voltage-gated Ca²⁺ channels (VGCCs) to the somatic Ca²⁺ transient during a single evoked AP. Bath application for 5–7 min of blockers for L-type (nimodipine, 10 μ M, $n=40$ single AP-induced Ca²⁺ transients from 5 neurons (40/5)), N-type (ω -conotoxin, 500 nM, $n=16/4$), or P/Q-type (ω -agatoxin, 50 nM, $n=15/3$) VGCCs decreased the Ca²⁺ transient ($\Delta F/F$)_{peak} associated with a single evoked AP with respect to control by 23% ($P < 0.05$), 24% ($P < 0.05$) and 14% ($P < 0.01$), respectively (Fig. 2A).

The effects of VGCC blockers on somatic Ca²⁺ transient amplitude suggest that Ca²⁺ transients are mediated by activation of VGCCs during APs. Would antagonizing these channels affect inspiratory drive potentials or inspiratory motor output in the XII nerve? To answer this, we measured the effects of 10 min bath application of nimodipine (10 μ M, $n=9$ slices), ω -conotoxin (500 nM, $n=4$) or ω -agatoxin (50 nM, $n=3$) (Fig. 2B). During this time frame, ω -conotoxin significantly decreased the interburst interval with respect

to control by 15% (from 7.4 ± 0.4 s to 6.3 ± 0.3 s; $P < 0.05$) (Fig. 2B). None of the VGCC blockers significantly affected the single neuron inspiratory drive amplitude or duration, or peak \int XII amplitude. However there was a clear tendency for ω -conotoxin to decrease inspiratory drive amplitude and duration, and for ω -agatoxin to increase inspiratory drive duration and interburst interval.

Somatic Ca²⁺ transients during inspiratory bursts

Somatic Ca²⁺ transients in active inspiratory preBötC neurons loaded with either Fluo-4 or OGB5N were seen only in response to APs (Fig. 3A). We did not detect any change in $\Delta F/F$ prior to the first AP of the inspiratory burst (Figs 3A, 4 and 5). Hyperpolarization of inspiratory neurons to eliminate endogenous APs resulted in a flat $\Delta F/F$ trace, i.e. there were no somatic Ca²⁺ transients associated with the inspiratory drive *per se* (Fig. 3Ab). Alternatively, we applied the Na⁺ channel blocker QX-314 (20 mM) in the intracellular pipette with either Fluo-4 ($n=4$ neurons) or OGB5N ($n=4$; data not shown). AP blockade was

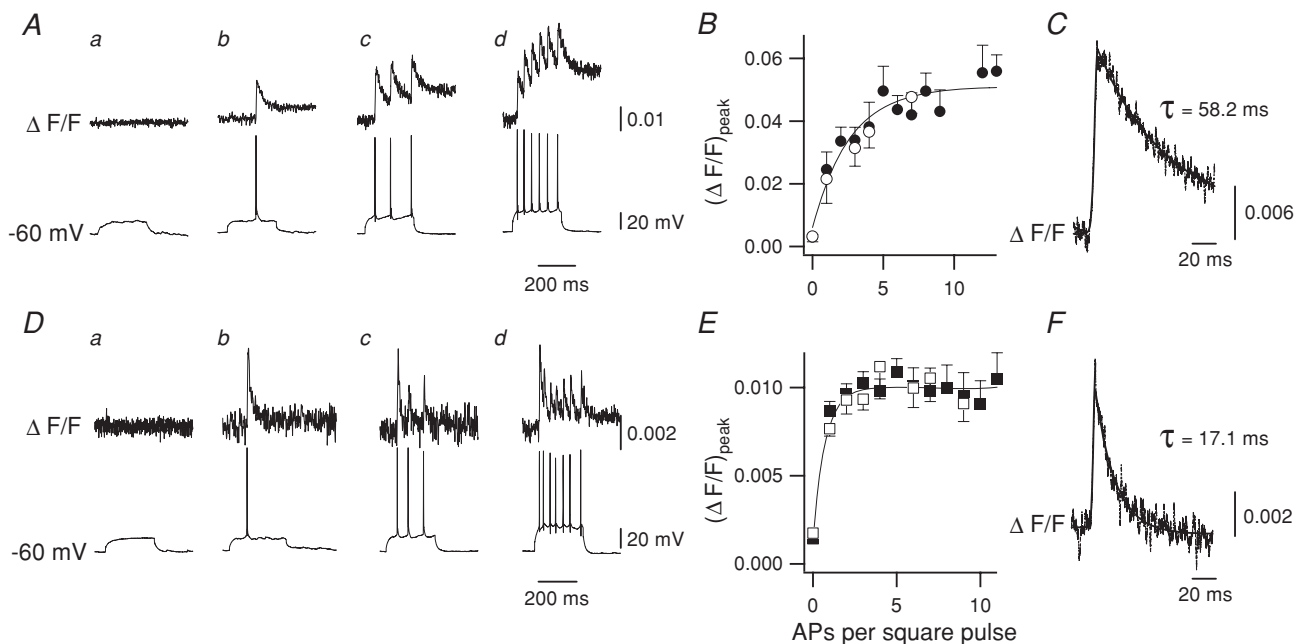


Figure 1. Somatic Ca²⁺ transients in response to evoked APs were measured in preBötC neurons after injection of depolarizing current (I_{DC})

A–C, characteristics of Ca²⁺ transients in neurons loaded with the high affinity Ca²⁺-sensitive dye Fluo-4. Aa–d, I_{DC} injected in interburst period of an inspiratory neuron ($V_m \approx -60$ mV). Somatic Ca²⁺ transients (upper traces) in response to evoked APs (lower traces). Ca²⁺ signals expressed as $\Delta F/F$. B, $(\Delta F/F)_{\text{peak}}$ values increase as a function of the number of APs. $(\Delta F/F)_{\text{peak}}$ fitted the same function in inspiratory ($n = 82$, ●) and non-respiratory ($n = 10$, ○) neurons. C, average single AP Ca²⁺ transient ($(\Delta F/F)_{\text{peak}} = 0.024 \pm 0.006$; $\tau = 58.2$ (ms)). D–F, similar to A–C, but neurons loaded with the low affinity Ca²⁺-sensitive dye OGB5N. Da–d, Ca²⁺ transients associated with each AP are readily observable. E, $(\Delta F/F)_{\text{peak}}$ values remained constant regardless of the number of evoked APs. $(\Delta F/F)_{\text{peak}}$ values fitted the same function in inspiratory ($n = 74$, ■) and non-respiratory ($n = 6$, □) neurons. F, average single AP Ca²⁺ transient ($(\Delta F/F)_{\text{peak}} = 0.0087 \pm 0.0005$; $\tau = 17.1$ (ms)).

achieved almost immediately after establishing whole-cell recording; small subthreshold potentials (4.8 ± 0.6 mV, 28.9 ± 2.2 ms) remained on top of each inspiratory envelope at a frequency of 33.8 ± 2.1 Hz. In neurons loaded with Fluo-4 and QX-314, the area of inspiratory drive potential ($n = 4$ neurons, 17 inspiratory drives per neuron) did not significantly change with respect to that in neurons loaded with Fluo-4 alone ($n = 4$ neurons, 20 inspiratory drives per neuron; $P = 0.08$). Under these conditions, somatic Ca²⁺ transients were not detected before or during inspiration, nor were they associated with subthreshold potentials (Fig. 3B). To test whether the somatic Ca²⁺ transient amplitude was proportional to AP amplitude, we bath applied TTX at low concentration (20 nM) to neurons loaded with either Fluo-4 ($n = 6$, Fig. 3C) or OGB5N ($n = 3$, data not shown) and current-clamped at $V_m = -40$ mV to facilitate AP generation. After 10 min, TTX increased the \int XIIIn interburst interval from 6.2 ± 0.9 s to 9.4 ± 3.8 s ($n = 6$ slices; n.s.) and decreased the \int XIIIn amplitude by 30% with respect to control ($n = 6$; $P < 0.05$, Fig. 3Cb). In the presence of TTX, the AP peak was 47.4 ± 0.6 mV above baseline and the amplitude of somatic single AP-induced Ca²⁺ transients was 55% smaller with respect to those in the absence of TTX ($n = 14$ AP-induced Ca²⁺ transients from 6 neurons (14/6), $P < 0.01$, Fig. 3Cb). TTX progressively decreased AP amplitude and completely abolished APs within 15 min ($n = 6$ neurons, Fig. 3Cc). No somatic Ca²⁺ transients were seen in the absence of APs.

To further examine whether somatic Ca²⁺ transients could be detected in preBötC neurons after the onset of the somatic inspiratory drive depolarization but before the first spontaneous AP, we aligned the first AP of multiple inspiratory bursts from neurons loaded with Fluo-4 ($n = 29$) or OGB5N ($n = 27$); we did not detect changes in averaged $\Delta F/F$ 200 ms prior to the first AP (Fig. 4A). In neurons loaded with Fluo-4 or OGB5N, the onset of the averaged somatic Ca²⁺ transient associated with the first AP was 1.7 and 2.2 ms, respectively, after AP onset (Fig. 4B). To test whether somatic Ca²⁺ increases during inspiration in the absence of APs, we aligned the first subthreshold transient potential on top of inspiratory drive ($n = 30$) of neurons loaded with Fluo-4 and QX-314; somatic Ca²⁺ signals were not detected before or during inspiration nor associated with transient subthreshold potentials (Fig. 4C).

To test our original hypothesis that somatic Ca²⁺ increases with inspiratory onset, we aligned the inspiratory drive onset of neurons loaded with Fluo-4 ($n = 29$), OGB5N ($n = 27$) or Fluo-4 and QX-314 ($n = 30$) and performed an analysis of variance of 20 ms $\Delta F/F$ segments before and after inspiratory drive onset on individual traces for each experimental group. If there were Ca²⁺ transients buried in the noise and not detectable in the

$\Delta F/F$, we would expect to see a change in the variance at inspiratory onset. No significant differences were found comparing the variance before and after inspiratory drive onset either in the presence or in the absence of APs (Fig. 5; $P = 0.94$, $P = 0.30$ and $P = 0.46$ for Fluo-4, OGB5N, and Fluo-4 and QX-314, respectively).

Discussion

In active preBötC inspiratory neurons, somatic Ca²⁺ transients occurred during the inspiratory burst, solely as the consequence of APs, which induced Ca²⁺ influx through VGCCs. In the absence of APs, the inspiratory drive potential was unaffected but somatic Ca²⁺ transients could not be detected, suggesting that these transients do not contribute to the inspiratory drive recorded in soma, the principal determinant for generation of APs.

Ca²⁺ contribution to inspiratory drive

Imaging of somatic Ca²⁺ transients in phase with preBötC neuron inspiratory activity has been used to

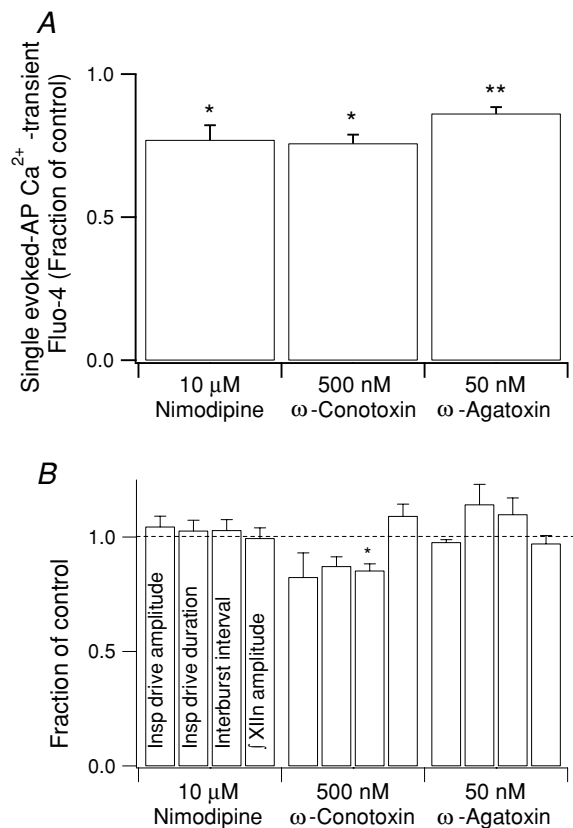


Figure 2. Effects of VGCC blockers

A, bath application for 5–7 min of VGCC blockers decreased the Ca²⁺ transient ($\Delta F/F$)_{peak} associated with a single evoked AP. Nimodipine: $n = 40$ transients from 5 neurons (40/5); ω -conotoxin: $n = 16/4$; ω -agatoxin: $n = 15/3$. B, effects of 10 min bath application of the VGCC blockers at the network level. Nimodipine: $n = 9$; ω -conotoxin: $n = 4$; ω -agatoxin: $n = 3$. * $P < 0.05$; ** $P < 0.01$.

study respiratory network connectivity, distribution and development (Koshiya & Smith, 1999; Thoby-Brisson *et al.* 2005; Barnes *et al.* 2007; Funke *et al.* 2007). Single neuron Ca^{2+} imaging has established that high voltage-activated (HVA) VGCCs are the dominant source of somatic Ca^{2+} in rhythmic respiratory neurons (Frermann *et al.* 1999). Activation of somatic TPRM4-like channels by Ca^{2+} is proposed as the mechanism that generates the inspiratory drive (Mironov, 2008). Here, using a faster detection system we show that, in the absence of APs, we could not detect somatic Ca^{2+} transients at any point in the respiratory cycle. We conclude that somatic Ca^{2+} signals seen in active preBötC neurons are due to somatic APs induced by the inspiratory drive potential, and not the inspiratory drive potential *per se*.

The synaptic currents that are the initiating source for the inspiratory drive potential are mainly the result of AMPA receptor activation (Greer *et al.* 1991; Funk *et al.* 1993; Morgado-Valle & Feldman, 2007). In preBötC

neurons, AMPARs almost exclusively contain the R-edited, non- Ca^{2+} permeable form of GluR2 (Paarmann *et al.* 2000), suggesting these receptors are not a source of Ca^{2+} influx. Another possible source of Ca^{2+} influx is through NMDARs. However in standard conditions *in vitro* these receptors appear activated but do not pass significant amounts of current due to their voltage-dependent Mg^{2+} block (Morgado-Valle & Feldman, 2007).

Source of Ca^{2+} transients

Somatic Ca^{2+} transients were seen only in response to APs. The onset of these Ca^{2+} transients had a minimal delay after the onset of APs (\sim ms), suggesting that intracellular somatic $[\text{Ca}^{2+}]$ rises due to a voltage-dependent, very rapid process rather than due to a slower process following activation of second messenger signalling cascades that release Ca^{2+} from intracellular stores. The contribution of Ca^{2+} -induced Ca^{2+} release to Ca^{2+} transients appears

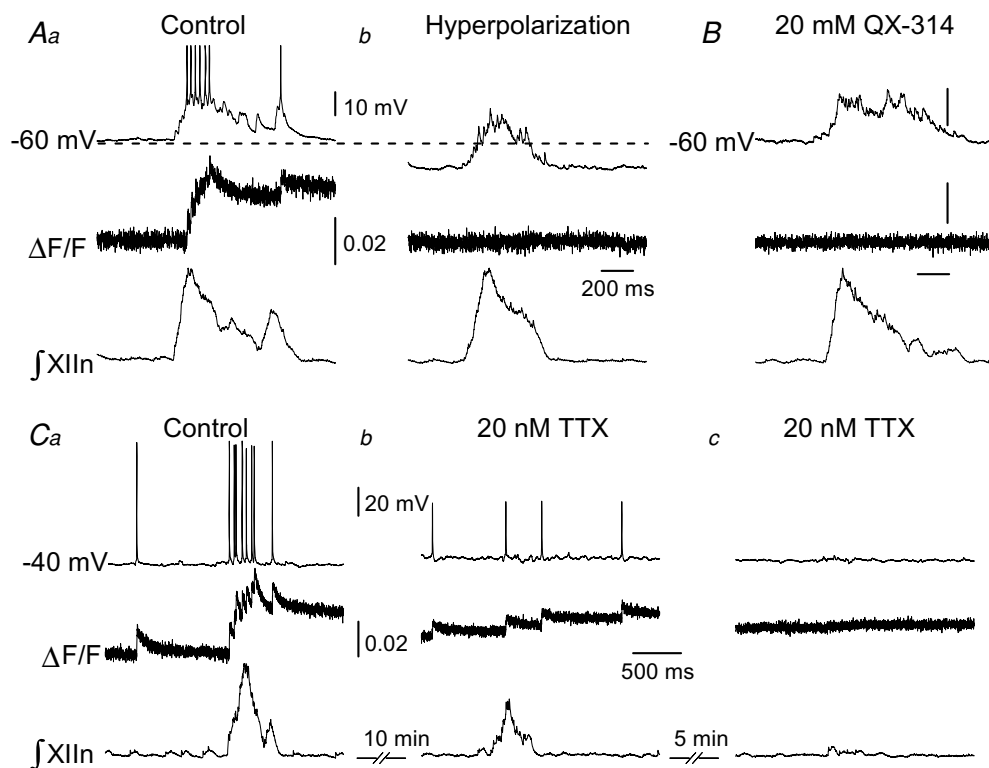


Figure 3. Somatic Ca^{2+} transients in active inspiratory preBötC neurons seen only in response to APs
Traces are: upper, current-clamped inspiratory neuron; middle, Fluo-4 Ca^{2+} signal expressed as $\Delta F/F$; lower, respiratory-related motor output recorded from XIIIn. *Aa*, $V_m \approx -60$ mV. $\Delta F/F$ did not change before 500 ms prior to the first AP. *Ab*, same neuron as in *Aa*. Hyperpolarization to eliminate APs produced a flat $\Delta F/F$ trace, i.e. no somatic Ca^{2+} transients. *B*, in neurons loaded with Fluo-4 and QX-314, no somatic Ca^{2+} transients were detected before or during inspiration, nor were any associated with subthreshold spike potentials. Representative trace. Scale bars as in *A*. $V_m \approx -40$ mV. Amplitude of somatic Ca^{2+} transients proportional to AP amplitude. *Cb*, same neuron as in *Ca*. After 10 min bath application of 20 nM TTX, AP peak only reached 47.4 ± 0.6 mV above the baseline and Ca^{2+} transients associated with APs were 55% smaller ($n = 14$ from 6 neurons; $P < 0.01$). *Cc*, TTX progressively decreased AP amplitude and completely abolished APs within 15 min ($n = 6$). No somatic Ca^{2+} transients were seen in the absence of APs.

to be more important in dendrites than in soma (Mironov, 2008). The overall role of Ca^{2+} -induced Ca^{2+} release on rhythmogenesis remains to be studied. In our experimental conditions, depletion of intracellular Ca^{2+} stores by bath application of the inhibitor of sarco/endoplasmic reticulum Ca^{2+} -ATPase thapsigargin ($20 \mu\text{M}$) did not have a significant effect on peak $\int \text{XII}$ amplitude nor on period (C. Morgado-Valle and J. L. Feldman, unpublished observations).

Abolishing APs either by hyperpolarization or Na^+ channel blockade eliminated somatic Ca^{2+} transients while the inspiratory drive potential was unaffected. This suggests that in active preBötC inspiratory neurons, where significant Ca^{2+} entry via ionotropic glutamate

channels appears to be unlikely, the main source of somatic Ca^{2+} influx is through activation of VGCCs during APs. Blockers of the high voltage-activated (HVA) L-, N- and P/Q-type VGCCs significantly decreased the peak somatic Ca^{2+} transient associated with single evoked APs. HVA VGCCs activate at or above -30 mV with peak conductance between 0 and $+10 \text{ mV}$ (Scott *et al.* 1991; Bertolino & Llinas, 1992). In rat preBötC neurons *in vitro* using a standard intracellular solution, the inspiratory drive amplitude is 5–20 mV above a baseline potential of -60 mV , well below that necessary to produce a significant current through HVA VGCCs. This suggests that, in the absence of APs, Ca^{2+} influx through somatic VGCCs does not contribute to the inspiratory drive potential.

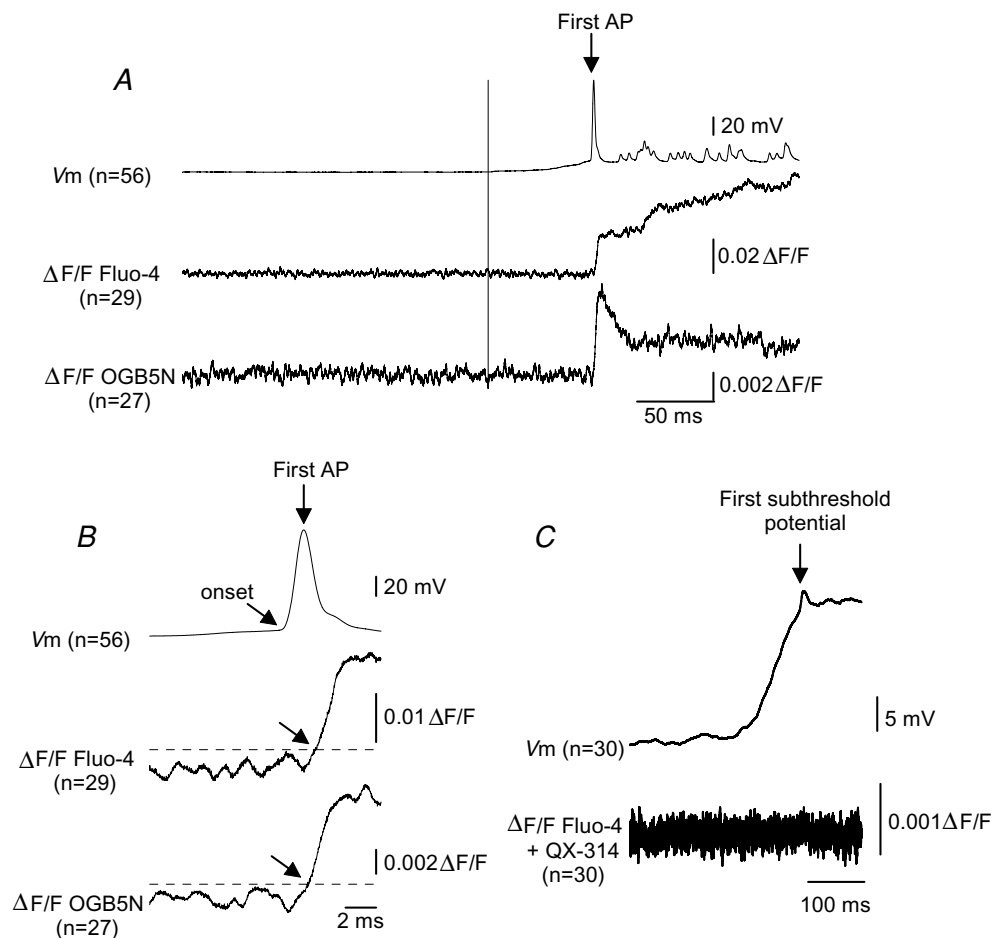


Figure 4. Somatic Ca^{2+} does not increase in the absence of AP

A, upper, average of superimposed inspiratory bursts from neurons loaded with Fluo-4 ($n = 29$), or OGB5N ($n = 27$) aligned to peak of first AP (arrow). Middle and lower, average $\Delta F/F$ of neurons loaded with Fluo-4 or OGB5N, respectively. We did not detect changes in averaged $\Delta F/F$ 300 ms prior to the first AP. B, upper, average AP from A. Lower and middle, average $\Delta F/F$ from neurons loaded with Fluo-4 (middle) or OGB5N (lower). Tilted arrows: AP and Ca^{2+} transient onset. Dashed line: three standard deviations of the mean baseline $\Delta F/F$. Time from AP onset to Ca^{2+} transient onset: 1.7 and 2.15 ms for Fluo-4 and OGB5N, respectively. C, upper, average of superimposed inspiratory drives ($n = 30$) from neurons loaded with Fluo-4 and QX-314, aligned to their first subthreshold spike potential. Lower, average $\Delta F/F$. Somatic Ca^{2+} signals were not detected before or during inspiratory drive nor associated with the first subthreshold spike potential.

However, AP-induced HVA VGCC Ca^{2+} transients can contribute to activation of Ca^{2+} -dependent channels such as large conductance (BK) and small conductance (SK) K^+ channels and/or TRPM4 and TRPM5 channels that are present in preBötC neurons and are proposed to shape the inspiratory drive (Pierrefiche *et al.* 1995; Bissonnette, 2002; Zhao *et al.* 2006; Crowder *et al.* 2007; Pace *et al.* 2007).

The low voltage-activated (LVA) T-type VGCC is proposed to underlie the depolarization seen in inspiratory neurons at inspiratory onset (Richter *et al.* 1993). LVA VGCCs activate at approximately -50 mV and reach maximum conductance between -40 and -10 mV (Scott *et al.* 1991; Bertolino & Llinas, 1992). At present we do not know their somatodendritic distribution in preBötC neurons. Since we did not detect any somatic Ca^{2+} transients in the absence of APs, either the Ca^{2+} influx through somatic T-type VGCCs is small or these channels are dendritic and produce transients that cannot be detected by our present methods.

Ca^{2+} -activated conductances

Ca^{2+} can play an essential role in termination of bursts of APs through activation of SK and BK K^+ channels (Richter *et al.* 1993). In many neurons these channels can influence firing through a close association with N- or L-type VGCCs or the NMDA receptor (Marrion & Tavalin, 1998; Shah & Haylett, 2002). In preBötC neurons neither

the somatodendritic distribution of these channels nor their association with VGCCs is known. Inhibition of BK channels reduces inspiratory burst frequency (Zhao *et al.* 2006) and can increase AP duration in preBötC neurons (Onimaru *et al.* 2003). We suggest that in preBötC neurons, Ca^{2+} -dependent K^+ channels are in the vicinity of VGCCs as occurs in other neuronal types (Womack *et al.* 2004; Goldberg & Wilson, 2005).

Ca^{2+} can also activate Ca^{2+} -activated Cl^- channels, affecting neuronal excitability and response to synaptic input and firing rate (Korn *et al.* 1991; Barnes & Deschenes, 1992). To date, we do not know whether these channels are present in preBötC neurons and, if so, how they shape APs and the inspiratory drive.

Somatic versus dendritic Ca^{2+} influx

Using a single photodiode approach, we did not detect somatic spontaneous non-AP evoked Ca^{2+} signals during or before the onset of inspiratory drive. However, while our approach has a higher temporal resolution, it has spatial resolution limitations when compared with other approaches, e.g. two-photon line scan microscopy. Given these spatial resolution limitations, we could not evaluate the role of dendritic Ca^{2+} fluxes, nor detect highly localized Ca^{2+} transients, such as those in microdomains near synapses. In proximal dendrites from single preBötC neurons, millisecond resolution Fluo-4 Ca^{2+} imaging (sampling rate = 1 kHz) with high spatial resolution (512×512 pixels) reveals AP-dependent Ca^{2+} transients ($\Delta F/F \sim 0.06$) during inspiration and AP-independent small ($\Delta F/F \sim 0.02$) Ca^{2+} transients preceding the onset of the first AP (C. Morgado-Valle and J. L. Feldman, unpublished observations). In slices bath loaded with Fluo-3 AM, two-photon imaging shows Ca^{2+} waves dependent on activation of metabotropic glutamate receptors; these dendritic Ca^{2+} waves are followed by somatic Ca^{2+} transients and are proposed to activate somatic TRPM4-like channels to promote generation of inspiratory bursts (Mironov, 2008). Using our high temporal resolution detection system in single neurons we did not detect somatic Ca^{2+} transients preceding the onset of inspiratory drive.

Intracellular iontophoretic injection of 5 mM BAPTA in late inspiratory neurons of the ventral respiratory column caudal to the preBötC (presumptively premotoneurons) in adult, anaesthetized, vagotomized cats increases AP frequency, whereas in postinspiratory neurons it increases both AP frequency and burst duration (Pierrefiche *et al.* 1995; Haji & Ohi, 2006). While comparison of these results with our present study may be confounded by anaesthesia, age and methodology, e.g. iontophoretic injection rather than passive diffusion, these results do suggest that Ca^{2+} dynamics in inspiratory premotoneurons is different from that of preBötC inspiratory neurons. Alheid *et al.*

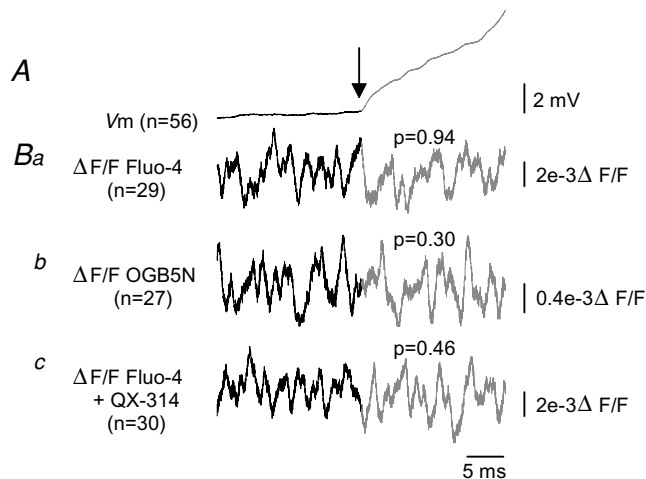


Figure 5. Somatic Ca^{2+} does not increase during inspiratory drive

A, average inspiratory drives from neurons ($n = 56$) loaded with Fluo-4 ($n = 29$) or OGB5N ($n = 27$) aligned to inspiratory drive onset (arrow). B, $\Delta F/F$ was computed for each of n traces (as indicated) from a single neuron, ± 20 ms of inspiratory onset, then averaged. Analysis of variance was performed on individual traces. There were no differences in variance before and after inspiratory drive onset in any condition (Student's t test). Ba, Fluo-4, $P = 0.94$; Bb, OGB5N, $P = 0.30$; Bc, Fluo-4 + QX-314, $P = 0.46$.

(2002) proposed precisely this possibility when they found that rat preBötC neurons lack expression of some of the most important endogenous Ca²⁺ buffering proteins that are nonetheless present in more caudal premotoneurons.

If somatic Ca²⁺ transients in preBötC neurons were crucial for generation of inspiratory drive, one would expect a rapid if not immediate effect after establishing whole cell recording conditions with a pipette containing 30 mM BAPTA on inspiratory drive amplitude, which is not the case (Pace *et al.* 2007). However, under these conditions there is a slow onset, i.e. several minutes, reduction in the amplitude of inspiratory drive, a time frame consistent with slow diffusion of BAPTA into distal dendrites; this delayed reduction in somatic inspiratory drive is postulated to be due to quenching of distal dendritic Ca²⁺ transients (Pace *et al.* 2007). We suggest that dendritic Ca²⁺ transients amplify synaptic currents with significant effects on somatic inspiratory drive potentials (Rekling & Feldman, 1998), as opposed to activating somatic currents.

In conclusion, in active preBötC inspiratory neurons, somatic Ca²⁺ transients do not significantly contribute to the inspiratory drive. We posit a critical role for dendritic Ca²⁺ transients in preBötC neurons in determining their excitability and ultimately their contribution to rhythm generation.

References

- Alheid GF, Gray PA, Jiang MC, Feldman JL & McCrimmon DR (2002). Parvalbumin in respiratory neurons of the ventrolateral medulla of the adult rat. *J Neurocytol* **31**, 693–717.
- Augustine GJ, Santamaria F & Tanaka K (2003). Local calcium signaling in neurons. *Neuron* **40**, 331–346.
- Barnes S & Deschenes MC (1992). Contribution of Ca and Ca-activated Cl channels to regenerative depolarization and membrane bistability of cone photoreceptors. *J Neurophysiol* **68**, 745–755.
- Barnes BJ, Tuong CM & Mellen NM (2007). Functional imaging reveals respiratory network activity during hypoxic and opioid challenge in the neonate rat tilted sagittal slab preparation. *J Neurophysiol* **97**, 2283–2292.
- Bertolino M & Llinas RR (1992). The central role of voltage-activated and receptor-operated calcium channels in neuronal cells. *Annu Rev Pharmacol Toxicol* **32**, 399–421.
- Bissonnette JM (2002). The role of calcium-activated potassium channels in respiratory control. *Respir Physiol Neurobiol* **131**, 145–153.
- Crowder EA, Saha MS, Pace RW, Zhang H, Prestwich GD & Del Negro CA (2007). Phosphatidylinositol 4,5-bisphosphate regulates inspiratory burst activity in the neonatal mouse preBötzing complex. *J Physiol* **582**, 1047–1058.
- Del Negro CA, Morgado-Valle C & Feldman JL (2002). Respiratory rhythm: an emergent network property? *Neuron* **34**, 821–830.
- Del Negro CA, Morgado-Valle C, Hayes JA, Mackay DD, Pace RW, Crowder EA & Feldman JL (2005). Sodium and calcium current-mediated pacemaker neurons and respiratory rhythm generation. *J Neurosci* **25**, 446–453.
- DiGregorio DA & Vergara JL (1997). Localized detection of action potential-induced presynaptic calcium transients at a *Xenopus* neuromuscular junction. *J Physiol* **505**, 585–592.
- Elsen FP & Ramirez JM (1998). Calcium currents of rhythmic neurons recorded in the isolated respiratory network of neonatal mice. *J Neurosci* **18**, 10652–10662.
- Feldman JL & Del Negro CA (2006). Looking for inspiration: new perspectives on respiratory rhythm. *Nat Rev Neurosci* **7**, 232–234.
- Frermann D, Keller BU & Richter DW (1999). Calcium oscillations in rhythmically active respiratory neurones in the brainstem of the mouse. *J Physiol* **515**, 119–131.
- Funk GD, Johnson SM, Smith JC, Dong XW, Lai J & Feldman JL (1997). Functional respiratory rhythm generating networks in neonatal mice lacking NMDAR1 gene. *J Neurophysiol* **78**, 1414–1420.
- Funk GD, Smith JC & Feldman JL (1993). Generation and transmission of respiratory oscillations in medullary slices: role of excitatory amino acids. *J Neurophysiol* **70**, 1497–1515.
- Funke F, Dutschmann M & Müller M (2007). Imaging of respiratory-related population activity with single-cell resolution. *Am J Physiol Cell Physiol* **292**, C508–C516.
- Goldberg JA & Wilson CJ (2005). Control of spontaneous firing patterns by the selective coupling of calcium currents to calcium-activated potassium currents in striatal cholinergic interneurons. *J Neurosci* **25**, 10230–10238.
- Gray PA, Janczewski WA, Mellen N, McCrimmon DR & Feldman JL (2001). Normal breathing requires preBötzing complex neurokinin-1 receptor-expressing neurons. *Nat Neurosci* **4**, 927–930.
- Greer JJ, Smith JC & Feldman JL (1991). Role of excitatory amino acids in the generation and transmission of respiratory drive in neonatal rat. *J Physiol* **437**, 727–749.
- Haji A & Ohi Y (2006). Ryanodine receptor/Ca²⁺ release mechanism in rhythmically active respiratory neurons of cats *in vivo*. *Neuroscience* **140**, 343–354.
- Kim AM & Vergara JL (1998). Supercharging accelerates T-tubule membrane potential changes in voltage clamped frog skeletal muscle fibers. *Biophys J* **75**, 2098–2116.
- Korn SJ, Bolden A & Horn R (1991). Control of action potentials and Ca²⁺ influx by the Ca²⁺-dependent chloride current in mouse pituitary cells. *J Physiol* **439**, 423–437.
- Koshiya N & Smith JC (1999). Neuronal pacemaker for breathing visualized *in vitro*. *Nature* **400**, 360–363.
- Ladewig T & Keller BU (2000). Simultaneous patch-clamp recording and calcium imaging in a rhythmically active neuronal network in the brainstem slice preparation from mouse. *Pflügers Arch* **440**, 322–332.
- Marrion NV & Tavalin SJ (1998). Selective activation of Ca²⁺-activated K⁺ channels by co-localized Ca²⁺ channels in hippocampal neurons. *Nature* **395**, 900–905.
- Mironov SL (2008). Metabotropic glutamate receptors activate dendritic calcium waves and TRPM channels which drive rhythmic respiratory patterns in mice. *J Physiol* **586**, 2277–2291.

- Mironov SL & Richter DW (1998). L-type Ca^{2+} channels in inspiratory neurones of mice and their modulation by hypoxia. *J Physiol* **512**, 75–87.
- Morgado-Valle C & Feldman JL (2007). NMDA receptors in preBötzinger complex neurons can drive respiratory rhythm independent of AMPA receptors. *J Physiol* **582**, 359–368.
- Onimaru H, Ballanyi K & Homma I (2003). Contribution of Ca^{2+} -dependent conductances to membrane potential fluctuations of medullary respiratory neurons of newborn rats in vitro. *J Physiol* **552**, 727–741.
- Onimaru H, Ballanyi K & Richter DW (1996). Calcium-dependent responses in neurons of the isolated respiratory network of newborn rats. *J Physiol* **491**, 677–695.
- Paarmann I, Freremann D, Keller BU & Hollmann M (2000). Expression of 15 glutamate receptor subunits and various splice variants in tissue slices and single neurons of brainstem nuclei and potential functional implications. *J Neurochem* **74**, 1335–1345.
- Pace RW, Mackay DD, Feldman JL & Del Negro CA (2007). Inspiratory bursts in the preBötzinger Complex depend on a calcium-activated non-specific cation current linked to glutamate receptors in neonatal mice. *J Physiol* **582**, 113–125.
- Pena F, Parkis MA, Tryba AK & Ramirez JM (2004). Differential contribution of pacemaker properties to the generation of respiratory rhythms during normoxia and hypoxia. *Neuron* **43**, 105–117.
- Pierrefiche O, Champagnat J & Richter DW (1995). Calcium-dependent conductances control neurones involved in termination of inspiration in cats. *Neurosci Lett* **184**, 101–104.
- Pierrefiche O, Haji A, Bischoff A & Richter DW (1999). Calcium currents in respiratory neurons of the cat in vivo. *Pflugers Arch* **438**, 817–826.
- Rekling JC & Feldman JL (1998). PreBötzinger complex and pacemaker neurons: hypothesized site and kernel for respiratory rhythm generation. *Annu Rev Physiol* **60**, 385–405.
- Richter DW, Champagnat J, Jacquin T & Benacka R (1993). Calcium currents and calcium-dependent potassium currents in mammalian medullary respiratory neurones. *J Physiol* **470**, 23–33.
- Ruangkittisakul A, Schwarzacher SW, Secchia L, Poon BY, Ma Y, Funk GD & Ballanyi K (2006). High sensitivity to neuromodulator-activated signaling pathways at physiological $[\text{K}^+]$ of confocally imaged respiratory center neurons in on-line-calibrated newborn rat brainstem slices. *J Neurosci* **26**, 11870–11880.
- Scott RH, Pearson HA & Dolphin AC (1991). Aspects of vertebrate neuronal voltage-activated calcium currents and their regulation. *Prog Neurobiol* **36**, 485–520.
- Shah MM & Haylett DG (2002). K^+ currents generated by NMDA receptor activation in rat hippocampal pyramidal neurons. *J Neurophysiol* **87**, 2983–2989.
- Smith JC, Ellenberger HH, Ballanyi K, Richter DW & Feldman JL (1991). Pre-Bötzinger complex: a brainstem region that may generate respiratory rhythm in mammals. *Science* **254**, 726–729.
- Tan W, Janczewski WA, Yang P, Shao XM, Callaway EM & Feldman JL (2008). Silencing preBötzinger Complex somatostatin-expressing neurons induces persistent apnea in awake rat. *Nat Neurosci* **11**, 538–540.
- Thoby-Brisson M, Trinh JB, Champagnat J & Fortin G (2005). Emergence of the pre-Bötzinger respiratory rhythm generator in the mouse embryo. *J Neurosci* **25**, 4307–4318.
- Vennekens R & Nilius B (2007). Insights into TRPM4 function, regulation and physiological role. *Handb Exp Pharmacol*, 269–285.
- Womack MD, Chevez C & Khodakhah K (2004). Calcium-activated potassium channels are selectively coupled to P/Q type calcium channels in cerebellar Purkinje neurons. *J Neurosci* **24**, 8818–8822.
- Zhao MG, Hulsman S, Winter SM, Dutschmann M & Richter DW (2006). Calcium-regulated potassium currents secure respiratory rhythm generation after loss of glycinergic inhibition. *Eur J Neurosci* **24**, 145–154.

Acknowledgements

This research was supported by NIH Grant HL-40959. C.M.-V. is a Parker B. Francis Fellow in Pulmonary Research (Francis Families Foundation, Kansas City, MO, USA).